Journal of Computer & Robotics Education Research (JOCRE)
Vol. 1, No. 1, 2024

Utilising a unique method to monitor Large Oil Storage Tanks' deformations via Interferometric Synthetic Aperture Radar (InSAR)

[1]Nwodo G.O., [2]Chiemela Victor Amaechi and [3]Alohan N.O

[1]Department of Geomatics, University of Benin, Benin City, Nigeria geoffrey.nwodo@uniben.edu

[2]Engineering Department, Lancaster University, Gillow Avenue, Bailrigg, Lancaster LA1 4YW, UK. chiemelavic@gmail.com

[3]Department of Geoinformatics and Surveying, Faculty of Environmental Sciences, University of Nigeria, Nsukka. alohannosakhare@gmail.com

Abstract

A method for monitoring the deformation of big oil storage tanks is proposed in this study. The method makes use of the Interferometric Synthetic Aperture Radar (InSAR) methodology. The purpose of this endeavour is to propose a solution that addresses the problem of oil spillage that occurs as a result of collapse of oil storage tanks. If massive oil storage tanks were to fail, it might have catastrophic consequences, including the loss of lives and property, the contamination of aquatic life, and the filing of lawsuits, among other things. Thus, the focus was on Forcados, Warri, Delta State, Nigeria as the location of the research area. The satellite imagery that were utilised were obtained from the Sentinel-1 Synthetic Aperture Radar (SAR) satellite hub of the European Space Agency (ESA) between 12-months period, covering the months of March 2017 until March 2016. In order to determine the state of these engineering structures and to identify any significant deviations from their original design, it is pertinent to perform periodic monitoring of these structures from time to time. For the detection of likely displacements as well as validating deformations measured upon the crude oil storage tank, a technology known as Small Baseline Subset Differential Interferometric Synthetic Aperture Radar (SBAS-DInSAR) approach was utilised. It was paired with an Object-Based Image Analysis (OBIA) approach to analyse the data. One of the 10 tanks that are located within the research area is used to illustrate the validation analysis. This tank is number seven. According to the findings, the horizontal distortions across the circular cross-section of the 7th Tank fall somewhere in a spectrum of -29.669mm and -3.131mm over the course of the study. An essential difficulty in engineering geodesy and one of the leading petroleum provinces worldwide is addressed by the efforts made herein, which offer a solution that is both practical and economically viable.

Keywords: Oil Storage Tanks, Synthetic Aperture Radar (SAR), Differential Synthetic Aperture Radar (DInSAR), Distortion, Deformation, Satellite Image; Monitoring

Introduction

Synthetic Aperture Radar (SAR) technology has seen increased use in monitoting deformation of engineering structures [1,2]. It has also been used to detect oil spills, river delineation, shoreline vulnerabilities in the Niger Delta using SAR imagery data [3-6]. Some of these oil spillages occur due to failure of the holding vessels, high environmental conditions and material failure of the oil storage tanks. An earlier study by Nwodo et al. [7] looked at the application of similar SAR imagery called Interferometric SAR (InSAR) in the Niger Delta area by looking at these structures that are holding the oil contents. Each of the large storage oil tanks have to be well designed to hold the content and support various loading and offloading operations. Figure 1 shows some large storage oil tanks in Mosimi depot, Ogun State, Nigeria.

Figure 1: Cylindrical Oil storage tanks in Mosimi Depot in Ogun State, Nigeria holding four oil products. Source: [8,9]

However, oil tanks can also be positioned in an array for storage of oil, such as the Mosimi depot in Ogun State of Nigeria that was constructed in 1978 and recommissioned in 2016 by Nigerian National Petroleum Corporation (NNPC) (see Figure 1). According to NNPC, the oil tank in this depot was stated to increase Nigeria's storage capacity for petroleum products by 87.7m liters [8,9]. When they reconstructed the depot's Tanks 22, 12 and 11 back in 2016, it eased the storage capacity with a combined increased volume at 54% of the total storage capacity of petrol (also called Premium Motor Spirit-P.M.S.) [8,9]. An article by Bloomberg [10] presented a recently constructed large storage oil tanks at Dangote Refinery in Lagos, Nigeria, which is designed to

hold 30,000,000 litres of gasoline. Within the Nigeria oil sector, various articles confirm that the use of these large oil storage tanks have seen increased use [7-10].

When large storage oil tanks fail, it almost always results in fatalities; hence, the safety of oil tanks including the contents of oil tanks is a problem for the industries that deal with the refinement of petroleum [11]. In the event that these tanks undergo even a little modification in terms of their shape and area, the integrity of these tanks could be jeopardised. Refineries and oil farms typically have massive storage tanks that are capable of holding a significant quantity of combustible and hazardous substances. It is common for any failure to result in a number of negative consequences, including environmental degradation, economic loss, threats to public health and safety, and legal action [12]. Since the discovery of crude oil in Oloibiri, Bayelsa State of Nigeria, in 1956, there has been a rise in the number of oil spills that have occurred in Nigeria [13]. There were a total of 784 oil spill occurrences that occurred between the years 1976 and 1980, which led to the loss of 1,336,875 barrels of oil [14]. This information has been gathered from observations or observations. In a similar vein, the oil spill that took place in Rivers State in 1970 was one of the most catastrophic environmental disasters that occurred in recorded history [14]. Texas Oil Company was responsible for the leak, which resulted in the dispersion of about 40,000 barrels of oil across the Delta region, resulting in the pollution of around 1,200 square kilometres. There were a total of 321 communities that were impacted by the oil spill, and an estimated 320,000 people were living in those villages. Approximately 180 people lost their lives as a result of this calamity, and there were 300 people who contracted various ailments as a result of consuming contaminated food and drinking dirty water [11,12].

In another recent study that was conducted on the subject of the causes of oil spills in Nigeria by recent researchers using SAR data also reflected a lot of oil spills were quantified in the Niger Delta region [5,6]. The failure of storage facilities has been shown to be the primary cause of oil spills in Nigeria between the years 1970 and 1998, according to previous research [12]. Storage tanks made of steel oil, particularly those that are between 15 and 20 years old, are at a considerable danger due to the age of the tank, its position, the state of the storage, the qualities of the soil, and other variables. Additionally, the non-uniform settlement of tank foundations, the entering and leaving of oil tanks, the loading and unloading of oil, plus the elevated temperatures of the crude will all produce stress on the membrane of the tank, which will result in the sediments settling [11]. The tanks in question consequently have a tendency to experience radial distortion. These oil storage tanks are regularly utilised for storing crude oil, which is the primary source of revenue for the economy of Nigeria [11,14]. Therefore, despite the risks and hazards that are involved, they continue to be used. Concerns have been raised about the structural deformation of these oil tanks on a consistent basis [15]. This is happening as a result of global warming as well as the rise in sea level that is related with storm surges. On top of that, the likelihood of these tanks breaking down is extremely high because of the inadequate monitoring, inspection, and maintenance procedures that are commonly used [14]. Detecting potential structural damage at an early stage is essential in order to prevent the severe repercussions that can result from tank failure. As a result, there is a requirement for a dependable system for monitoring the structural deformation of tanks on a routine basis.
A number of different techniques, including geodetic measurements, photogrammetry, and laser scanning (ALS), have been utilised in the past [16]. On the other hand, these techniques are not only expensive and time-consuming, but they are also rigorous and require some critical interpretation in order to reach the desired outcomes [17]. In addition, one of the most significant challenges that engineering geodesy faces is the construction of mathematical models (for

geodetic approach) that will reveal the properties of the deformation [7,13,14,]. Increased opportunities for Differential Interferometric SAR (DInSAR) applications are currently available as a result of the recent arrival of satellite constellations that deliver high-resolution SAR images (for example, Sentinel-1 satellite remote sensors). These applications have the ability to detect surface changes alongside fine spatial information as well as having shorter revisiting times [7,18,19]. Aside from that, there are various theories like the scale-space theory that is used to detect and analyse satellite images [20], also considered.

Therefore, the purpose of this research is to investigate the monitoring of large oil storage tanks utilising the DInSAR technology against the radial displacements and determining the health state of these tanks. This strategy takes advantage of the potential that is provided by Sentinel-1 SAR satellites in order to overcome the deficiencies that are currently present in conventional geodetic methods. The use of the InSAR approach has been identified as useful data source, which we have applied to create a system that is dependable and robust, as well as cost-effective for monitoring the structural performance of the large oil storage tanks. Thus, in order to address the problem of oil spills in Nigeria, which is caused by the collapse of big oil storage tanks as well as engineering facilities, we propose this solution. The processing technologies that were utilised were the Geographic Object Based Image Analysis (GEOBIA) Techniques and the Small BAseline Subset - Differential Interferometric Synthetic Aperture Radar (SBAS-DInSAR) Techniques. Our efforts have resulted in the development of a sustainable solution that addresses a significant problem in the oil industry of Nigeria. This is accomplished by lowering the costs, rigours, and time limits associated with the traditional approaches that are now in use.

Materials and Methods

The Study Area

This research was conducted by focusing on Forcados, which is located in the Warri South Local Government Area of Delta State, Nigeria. It was considered as the locality that is being investigated because it holds a resourceful oil terminal (see Figure 2). The coordinates for its location are as follows: latitude 5˚ 20’ 01”N, longitude 5˚ 21’ 30”E, and atitude 5˚ 20’ 56”N, longitude 5˚ 20’ 32”E. Ajidubu, Jala, Madagho, Ogidigben, as well as Ugborodu, are some of the communities that are located approximately 120 kilometres to the south-east of this location [7]. As a consequence of the fact that Forcados is one of the most significant petroleum provinces in the world, the geographic region has been the subject of much research (see Figure 3). Shell and Chevron, two of the most prominent multinational corporations, have their headquarters there. Operationally, Ogidigben, Otumara, as well as Sagara, are the names of the flow stations that Shell operates in Escravos. Chevron, on the other hand, establishes its flow station offshore [7]. Strong wave activity alongside tidal currents are two characteristics that can be found in the Escravos River and its surrounding area. On the beach ridge, there is a significant amount of soil formation and plant growth. There are clear challenges involved in determining the path of the pipeline due to the presence of mangrove marshy swamps and creeks that cross each other numerous times. Also, the Forcados River makes connections between the Warri River and the Burutu Channel as well as other settlements along the tributaries plus terrains as seen in Figure 3.

Figure 2: The Forcados Terminal in Nigeria surrounded by walls

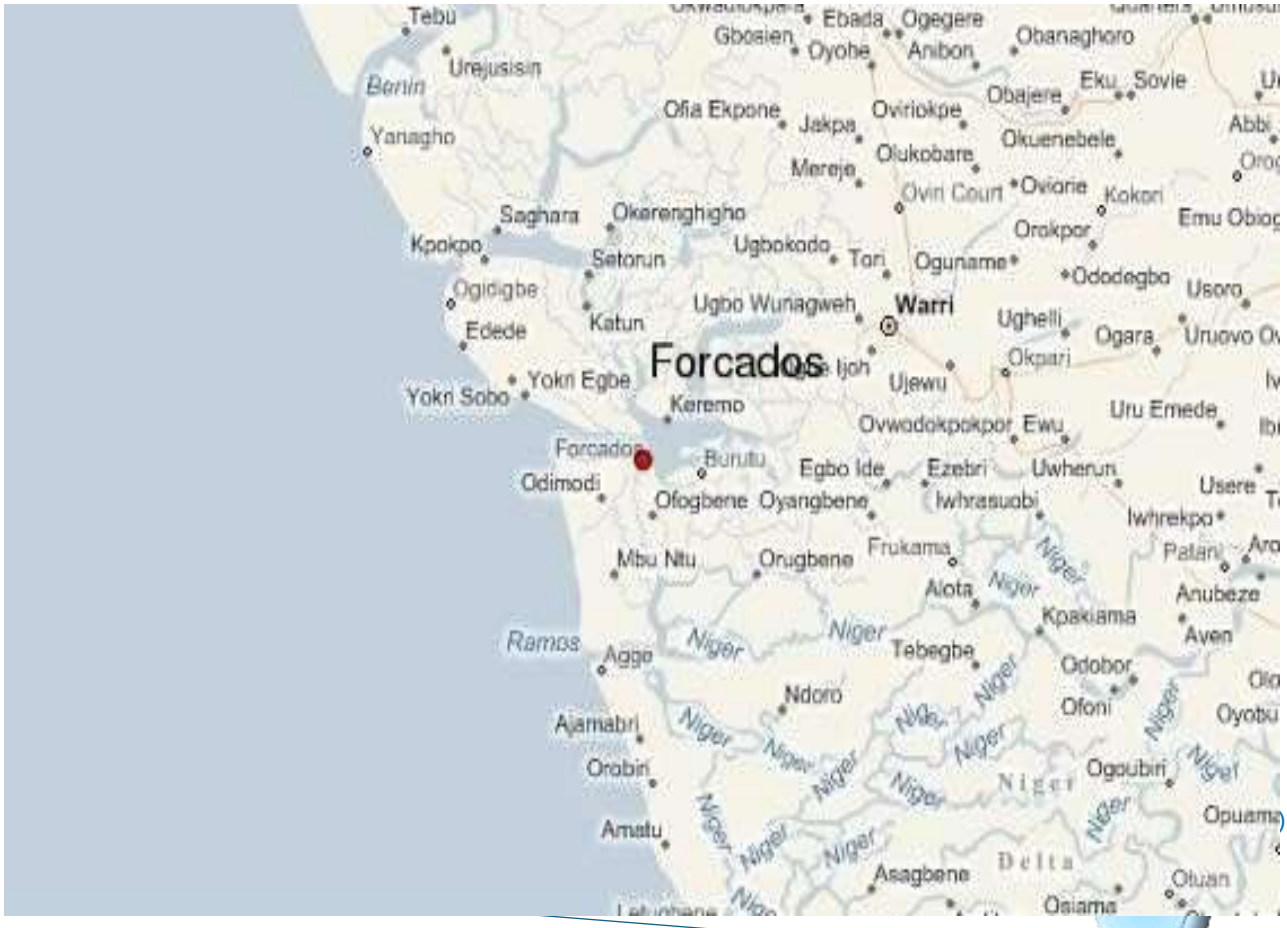

Figure 3: Map of Forcados Terminal in the Niger Delta showing the communities (Source: Map Data via Google)

Primary Data

The Copernicus Sentinel-1 Earth Observation Satellite SAR Data Archives provided the primary dataset that was utilised in this investigation. On the 6th of March 2017 and the 11th of March 2016, Sentinel 1 SAR images were taken using the Terrain Observation with Progressive Scans SAR (TOPSAR) and Single Look Complex (SLC) techniques. Both of the photographs that were used had a combined size of around 9.3 gigabytes, with each image having a size of approximately 4.6 gigabytes. (please refer to Figure 4A).

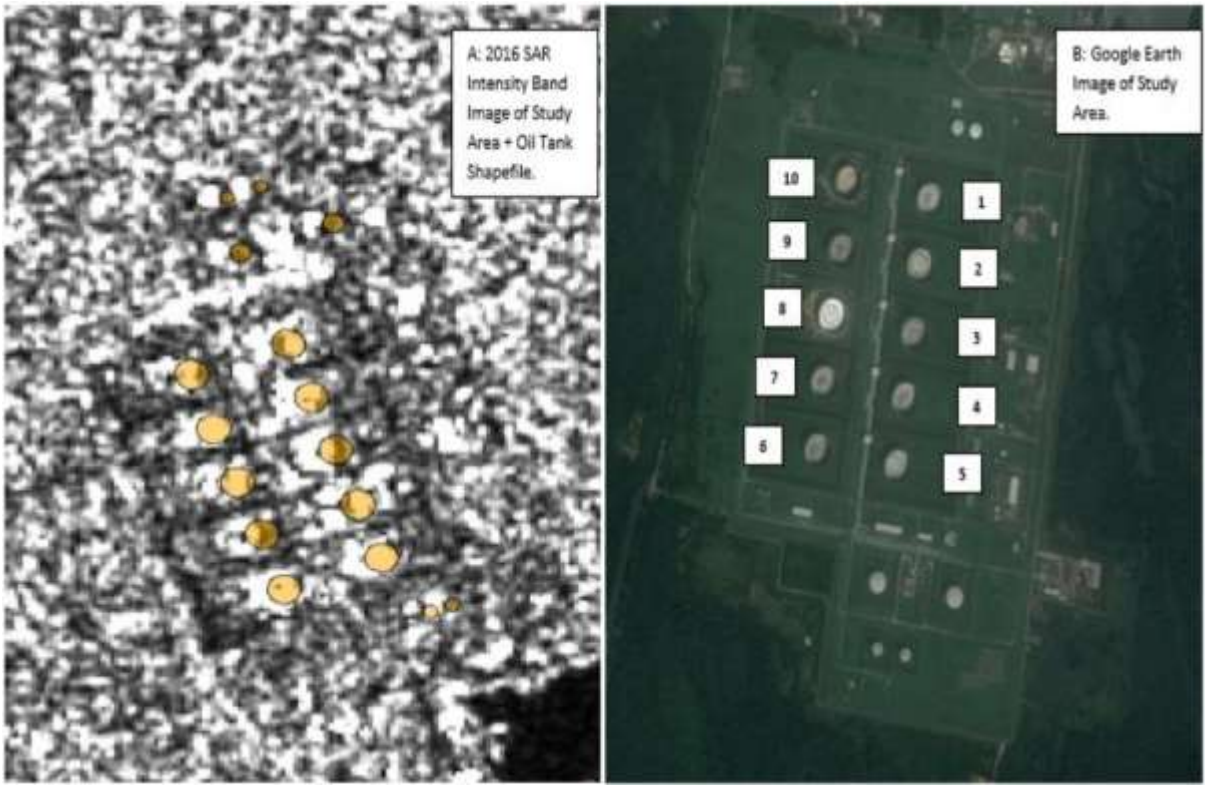

Figure 4: (A) the Sentinel-1 SLC SAR data along with the reference shapefile of the tanks containing oil, while (B) the Study Area, showing the tanks as located from Google Earth.

Data Validation

For the purpose of determining the existential accuracy evaluation within the oil storage tanks, an Object-based Image Analysis (OBIA) approach was utilised to validate the results of the deformation velocity measurements. It is necessary to have secondary reference data in order to carry out object-based accuracy assessment and validation of the final deformation outcome in accordance with our goals.

(1) traditional geodetic (X,Y,Z) field measurements of STUD locations on the storage tanks utilising a reflectorless total station instrument and

(2) vector shapefile derived from digitising the oil storage tanks from a 2m high-resolution Google Earth images of this study area were used to acquire the reference data.

Both of these methods were utilised to acquire the reference data. In this study, the existential accuracy assessment was utilised as the accuracy assessment metric in order to validate the outcomes of the deformation [7,21,22,23]. Specifically, this is an object-level validation of the oil tank deformation, which is something that our research is interested in. The existence of the distortion within the oil tanks may be determined with the help of the existential accuracy, which helps to determine whether or not one exists. It was determined that there are two accuracy indicators that pertain to the presence of deformation within the oil tanks.
(a) The first of these is the true positives (TP); these are instances in which distortion is present in the polygon reference layer (the shapefile of oil tanks), as such deformation exists.
(b) The second of these is the false negatives (FN); these are instances in which the polygon reference layer (the shapefile of oil tanks) fails to recognise deformation. This is referred to as a failure to identify deformation.

Due to the fact that we were more concerned with the deformation that occurred within the tanks, we chose to disregard false positives, which pertain to the inaccurate detection of deformation that does not exist in the polygon reference layer. Because of this, we derived the reference datapoint from tanks that were not connected to any other tanks. Trying to make computations via the false positives will result in a biassed result. An illustration of an OBIA existential accuracy measurement is shown in Figure 5, which is used to detect whether or not there is deformation within the oil tanks.

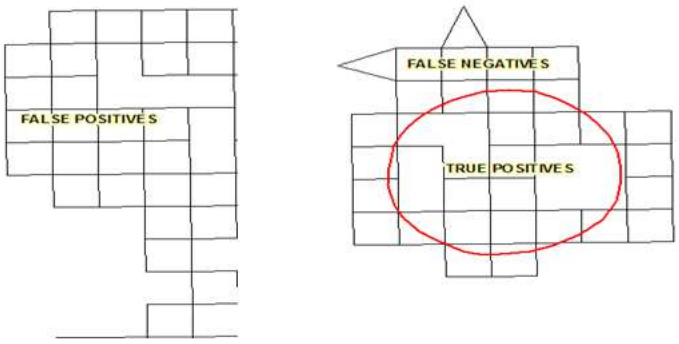

Figure 5: An illustration of an OBIA existential accuracy measurement used to detect whether or not there is deformation within the oil tanks.

Methodology

There were six distinct steps that were involved in the development of the methodology that was used to derive deformation measurements on crude oil storage tanks including the following, as illustrated in Figure 6.

(i) The first step is to download the Sentinel-1 SAR photos of the area under examination. The dates have a temporal variance of one year, and they are the 6th of March 2017 and the 11th of March 2016.

(ii) The SBASDInSAR Technique should be used to process the Sentinel-1 photos that have been downloaded.
(iii) The generation of horizontal deformation and time-series data based on the processed Sentinel-1 SAR images is the third step.

(iv) Create and import a tank shapefile coordinate by utilising a high-resolution Google Earth image of 2 meters (this is helpful for checking).

(v) In order to validate and evaluate the accuracy of the radial deformation of the tank's circular cross-section, it is necessary to carry out an Object-Based Image Analysis (OBIA).

(vi) Apply statistical regression analysis to the result of the deformation in order to determine whether or not there has been any change in the pattern or trends of the deformation.

The SBAS-DInSAR technique for the processing of data.

For the purpose of processing the Sentinel-1 SAR images, the researchers in the present study utilised a parallel computing approach presented in [7,28] known as the Small-Baseline Subset (SBAS-DInSAR). This technique was chosen from among various DInSAR techniques. The supervised implementation of the SBAS-DInSAR processing chain is depicted in Figure 6.

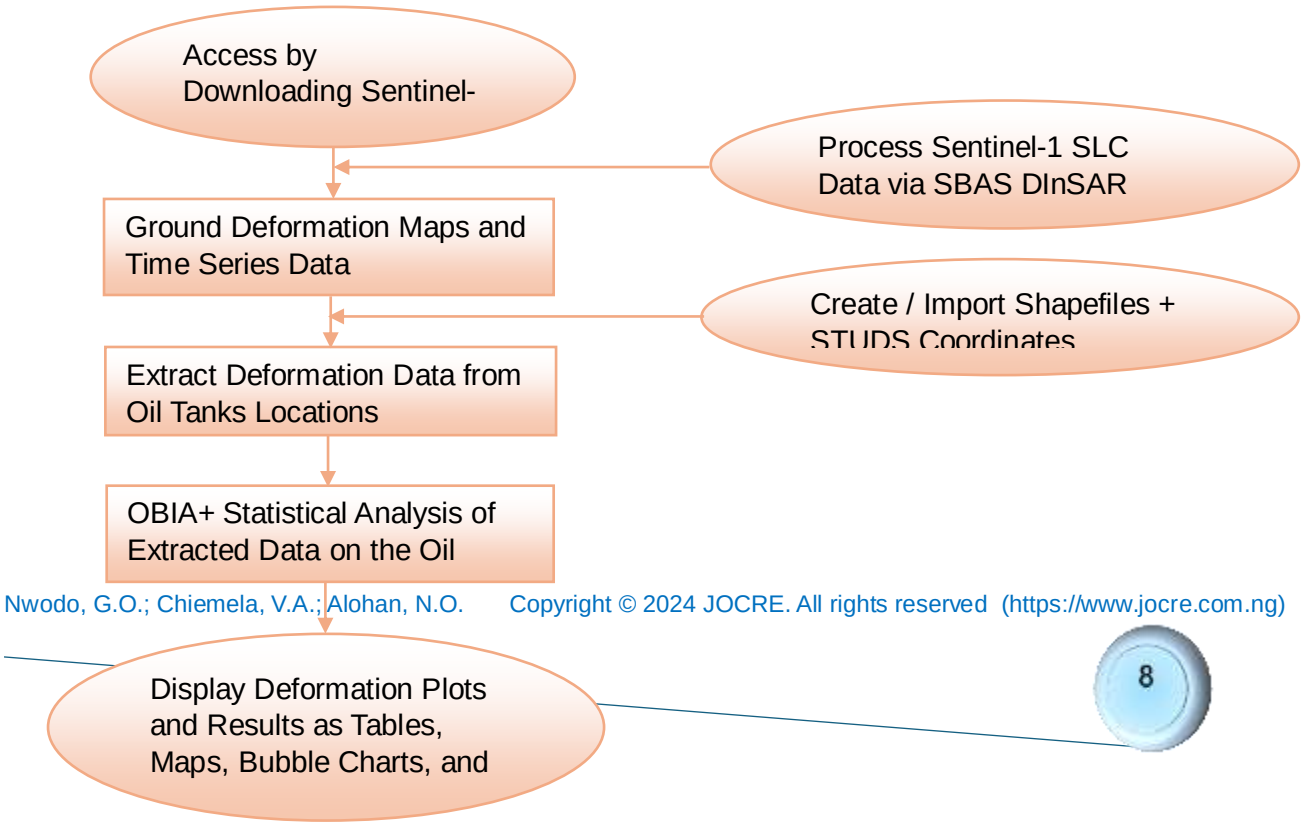

Figure 6: The flowchart for the methodology

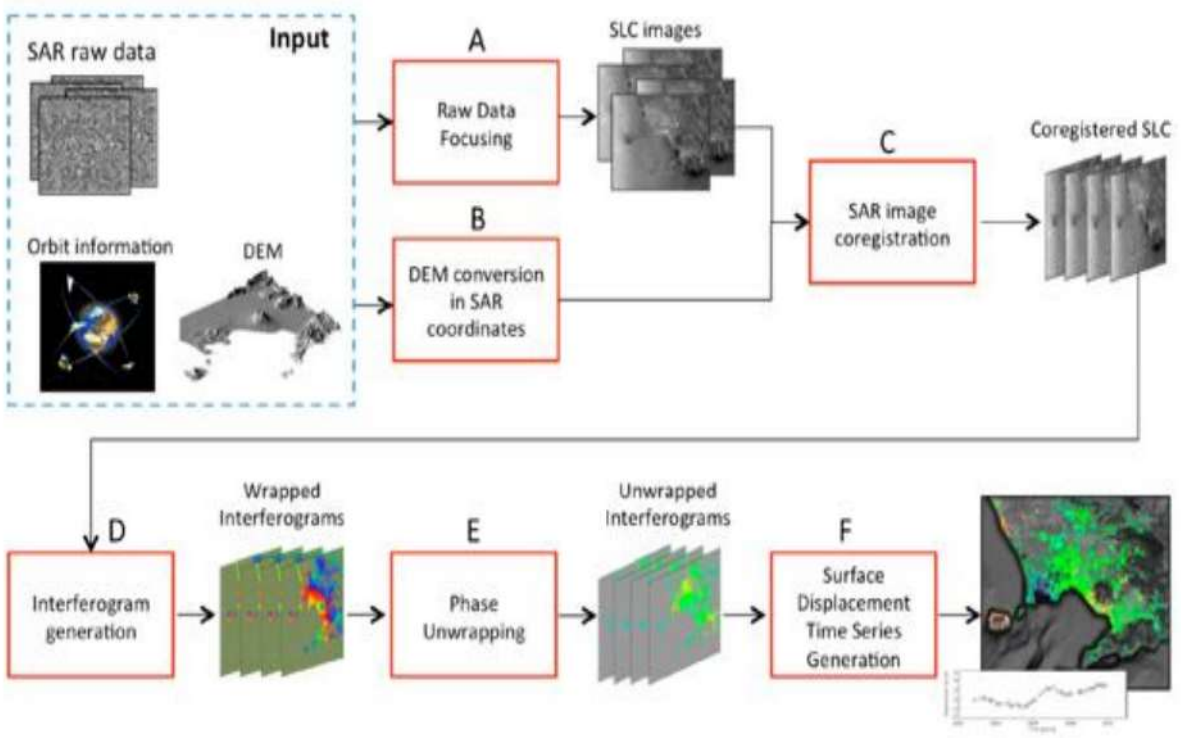

Figure 7: A supervised implementation of the SBAS-DInSAR processing chain (sources: [7,18]).

A sophisticated DInSAR processing chain is utilised in this method for the purpose of generating Earth deformation time series (TS) along the satellite line of sight (LOS) and estimating the mean yearly velocity maps (in millimetres per year) with millimetric precision [7,18]. In the SBAS-DInSAR workflow, the inputs consist of the SAR raw data that was acquired by the satellite over the same region and from the same look angle (same acquisition geometry). Additionally, the SBAS-DInSAR workflow takes into account the orbital information that indicates the position of the satellite throughout the acquisition time, as well as the Digital Elevation Model (DEM) of the area that was investigated. It is necessary for the SAR raw data to go through a particular processing (SAR focussing) in order to be converted into the appropriate radar image, which is referred to as Single Look Complex (SLC). This processing is shown in Block A of Figure 7. In their capacity as complex entities, SLCs are made up of amplitude and phase, with the latter characteristic serving as the foundation of the SAR interferometric process. In order to ensure that the phase contributions that are associated with each pixel of each image are correctly combined, it is necessary for all of the SLCs to be referred to the same spatial grid, which is referred to as the master. This technique, which is known as co-registration, is carried out by using geometric considerations that are based on the satellite orbital information and the digital elevation model (DEM) of the area. For this

reason, the DEM needs to be translated into the SAR geometry in the correct manner (as shown in Block B of Figure 7), so that it may be utilised appropriately in the subsequent step of co-registration (which is shown in Block C). Following the completion of the co-registration process, the SLCs are able to be coupled in what are known as interferometric pairs. These pairs are chosen from among all the available couples based on a minimal baseline criterion. The spatial and temporal baselines are the orbital and time separations between two SAR images, respectively. After that, the differential interferometric phase, also known as the interferogram, is retrieved from the image pairs in question. It has been established that the ground displacement that took happened in the time interval between the two SAR images is directly proportional to the phase difference that was observed [7,23]. In order to obtain the complete evolution of the phase difference, which is referred to as the wrapped phase, it is necessary to unwrap it. Such procedure, referred to as phase unwrapping, as carried out within block E through employing the Extended Minimum Cost Flow (EMCF) phase unwrapping algorithm [7,18,23]. On the unwrapped interferograms, a process is carried out in order to determine the residual topography phase component that may be caused by DEM mistakes. An methodology known as the least squares method is utilised in the execution of this operation [7,23].

Next comes the phase of estimating the residual topography, which comes before the final retrieval of the displacement time series (Block F), which is carried out at the pixel level. The number of SAR acquisitions that were employed for the interferometric analysis corresponds to the phase velocities that were measured between acquisitions that were time adjacent to one another. In general, the processing of DInSAR calls for some competent user inputs and evaluations in order to improve the quality and reliability of the DInSAR findings that are generated [7,18,23].

Geographic Object-Based Image Analysis (GEOBIA)

It has been argued that Geographic Object-Based Image Analysis (GEOBIA) is probably one of the solutions to deal with the limits and constraints that are associated with pixel-based image analysis [7,24]. This concept has further developed and gained widespread support. Segmentation, feature extraction, and edge detection are some of the older techniques that are used in remote sensing image analysis. GEOBIA is an extension of these approaches. Remote sensing imageries or thematic outputs are partitioned into areas or objects in this procedure, and then their attributes are analysed at various scales [7,24]. This method is implemented in order to achieve the desired results. During the processing of items, this method takes into account the temporal, spectral, and geographic features of such objects. Additionally, it offers the capability to query and link certain objects [7,25].

As a result of the fact that the picture-object is the fundamental methodological element and the focus of inquiry when object-based image analysis is being used, image context is extensively documented for object recognition [7,26]. In the process of classification, this is quite helpful in overcoming uncertainties that are brought about by a lack of evidence. GEOBIA is a technique that is very useful in capturing accurate information [7,27]. This technique

is particularly useful in situations when spectral features are not unique, but shape and neighbourhood interactions are distinct. One example of the supervised implementation of the GEOBIA technique is shown in Figure 8.

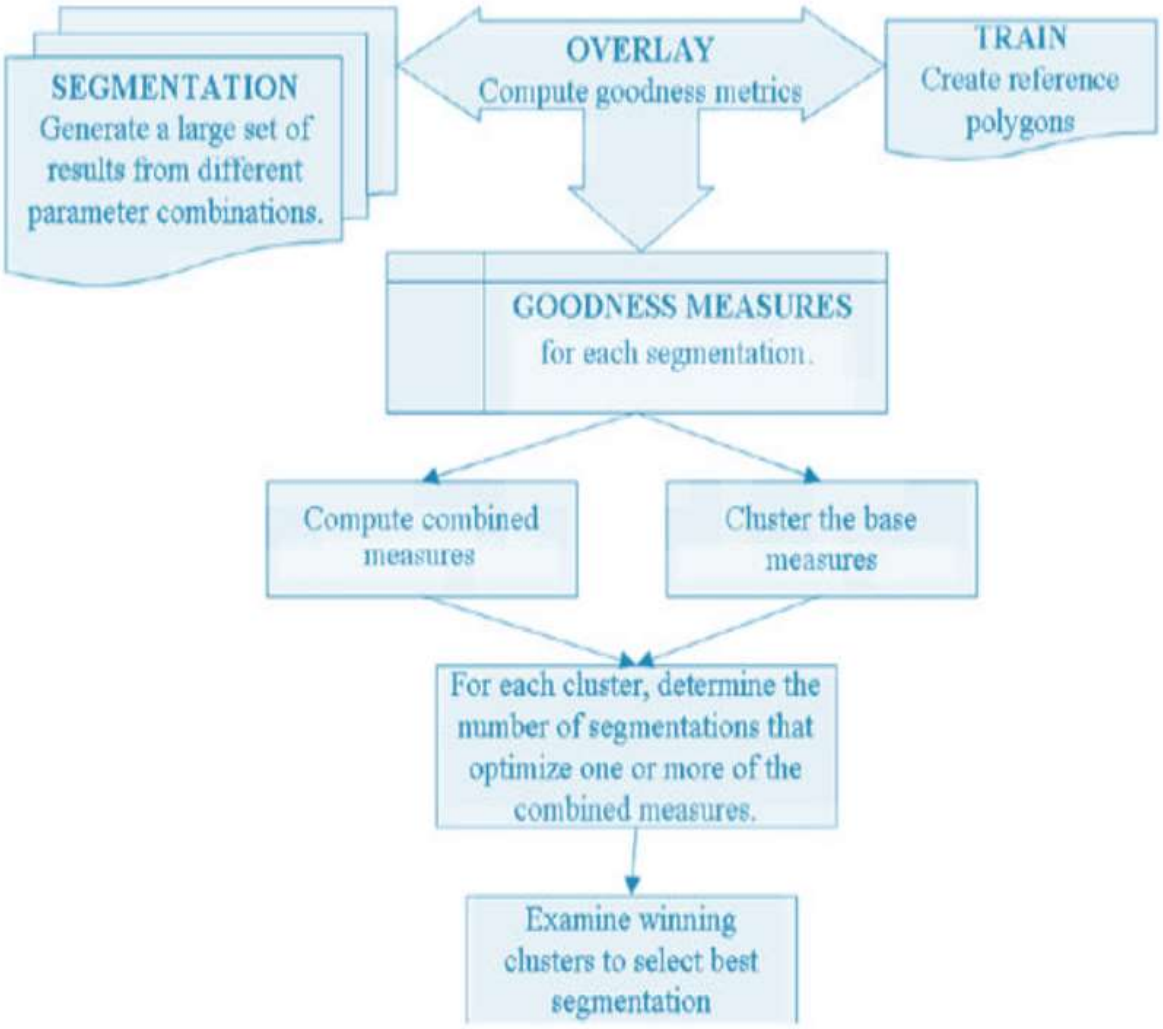

Figure 8: An example of the supervised implementation of the GEOBIA technique (source: [14]).

To create a more accurate representation that will result in enhanced repeatability while simultaneously lowering labour subjectivity and time expense, the primary objective of GEOBIA is to incorporate the concept of human visual perception of objects either during or after the categorisation process [24]. During the GEOBIA process, image segmentation plays a significant part. During this process, features are extracted with respect to their numerous qualities in order to differentiate one region from another geographical area.

Results and Analysis

Although there were ten tanks inside the study area (as shown in Figure 4), we restricted our validation investigation to include tank 7 for the purpose of this research. A horizontal deformation velocity map (millimetres), a coherence image map, segmentation findings, and a time series plot displaying a trend comparison between our deformation results using (DInSAR) and the classical geodetic insitu measurements are those that are included in the results.

The Results of the Vertical Deformation

Following the conversion from the residual phase correction to the phase to deformation (Figure 7), masking the area of low coherence, and geo-coding the products to have absolute geographical locations, the vertical deformation maps for each and every InSAR pair were ultimately obtained. Figure 9 is a representation of the vertical deformation map that may be found on Google Earth.

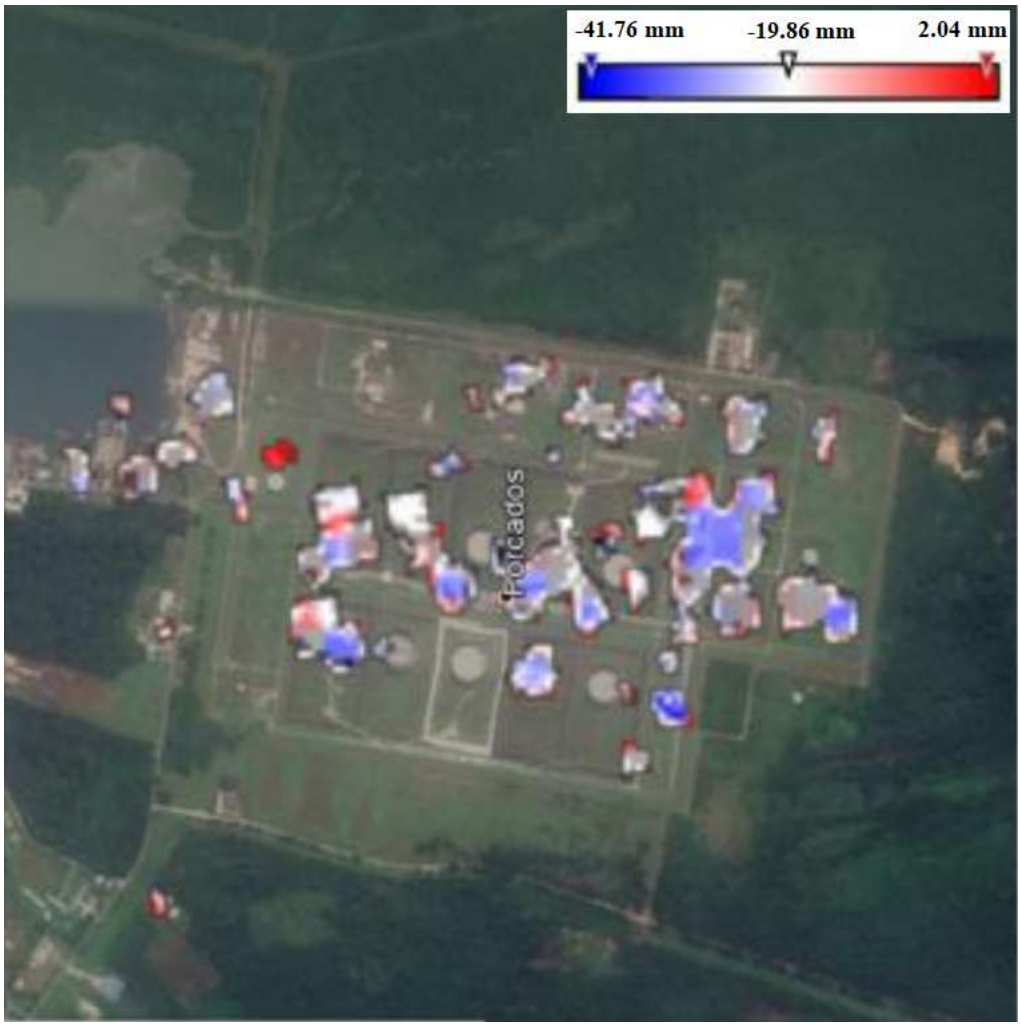

Figure 9: Representation of the vertical deformation map that may be found on Google Earth.

There are some tanks that have been affected by deformation, as shown in Figures 6 and 7, but there are other tanks that may not have been damaged at all. By measurements, the range of deformation that can occur is 2.04 millimetres to -41.76 millimetres. The displacement is classed using three different colours (red, white, and blue) according to the degree of deformation that occurs within each pair. These colours indicating high risk, medium risk, and low risk deformations, respectively, respectively, are used to classify the displacement. The vertical deformation of oil storage tanks is depicted in Figure 10, which also includes a matching shapefile.

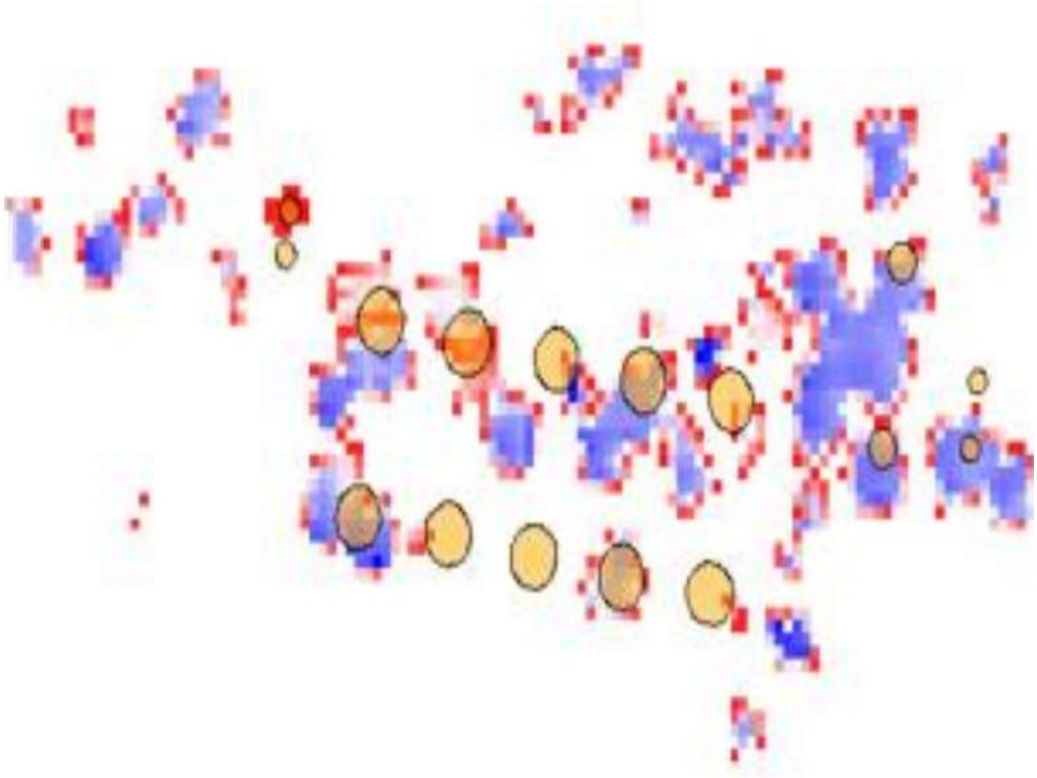

Figure 10: The matching shapefile alongside the horizontal deformation of oil storage tanks.

The Results of the Coherence Image

It has been demonstrated that the consistency of the subsidence zones has a direct bearing on the accuracy of the ground subsidence values that are monitored [28]. It is for this reason that the coherence between the reference image and the secondary image is evaluated as a measure of the quality of the phase information [29]. Interferometric processing can be performed on the pictures if they share significant similarities, which means that they are suitable for use. An overlay of the shapefile of oil storage tanks is shown in Figure 11, which depicts the coherence image from March 2017 to March 2016.

Though, in Figure 11, the coherence image for the period of March 2017 to March 2016 is displayed with intensity levels ranging from 0 to 1. The high-quality pixels with the black pixels display an intensity of 0 (no distortion), whereas the white pixels display an intensity of 1 (deformation). There is a possibility that deformation occurred in around twelve of the sixteen tanks that were displayed.

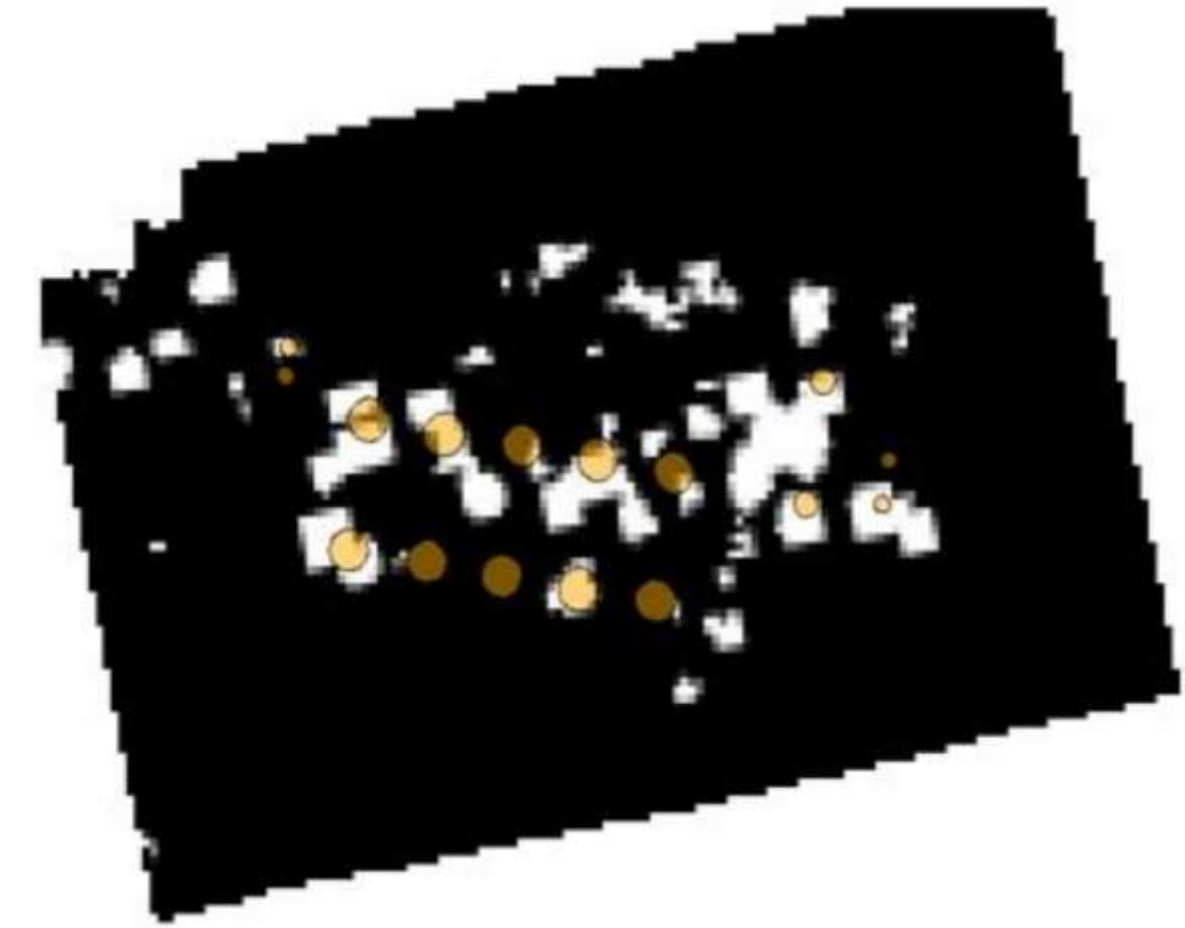

Figure 11: An overlay of the shapefile of oil storage tanks, which depicts the coherence image from March 2017 to March 2016.

Evaluation of the Segmentation

In GEOBIA, where features are retrieved with respect to their numerous qualities in order to differentiate one region from another, image segmentation plays a significant role in the process. In our approach, the results of the deformation map were partitioned into raster objects, also known as segments, by employing a region expanding segmentation technique as a post classification procedure (see Figures 12 and 13). in order to get rid of the false positives and keep the actual positives (as in Figure 12), It was necessary to trim the segmented deformation image of the research area (Figure 13) The true positives segmented deformation image is superimposed with a shapefile of crude oil storage tanks, as seen in Figure 12. An existential analysis was performed on the theme object that was constructed as a result.

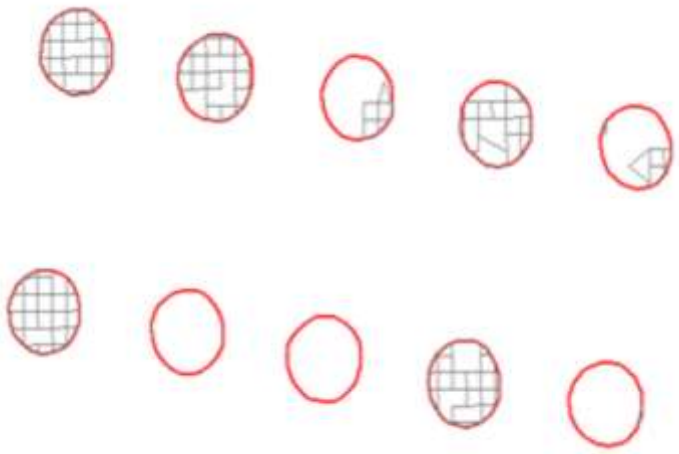

Figure 12: The true positives segmented deformation image is superimposed with a shapefile of crude oil storage tanks.

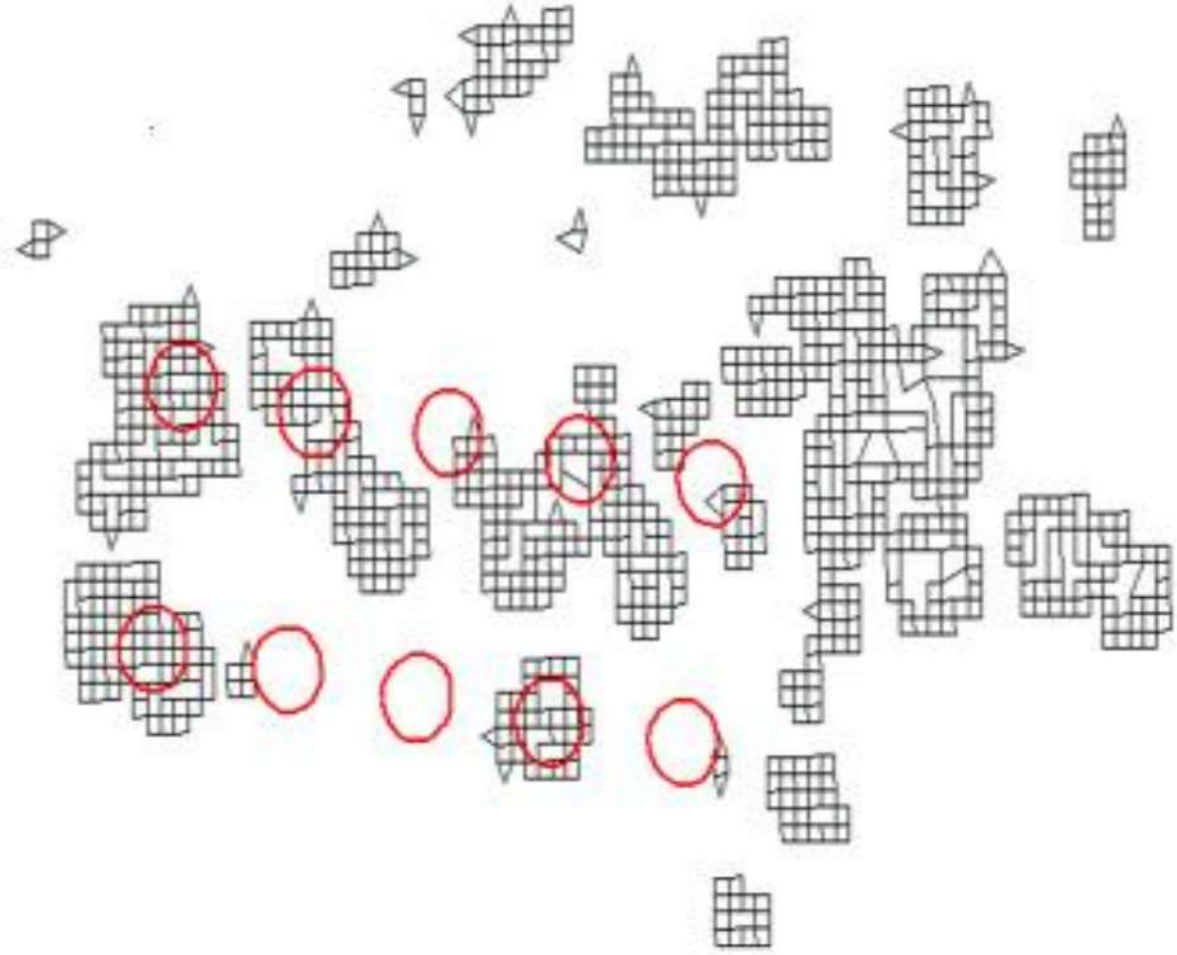

Figure 13: A segmented deformation image of crude oil storage tanks is superimposed on top of a shapefile.

Extracting Deformation Values.

In order to extract the deformation values from the DInSAR processed image, the XYZ survey points that were observed from the STUD and were located on the oil storage tanks were imported and employed. In order to verify the observation points (STUD) along the monitoring findings of the deformation image (as in Figure 14), the subsequent steps were taken. The image of the deformation of Tank 7 with STUD (12) captured around the crude oil storage tanks is shown in Figure 14. For the purpose of statistical analysis, these retrieved deformation values were utilised.

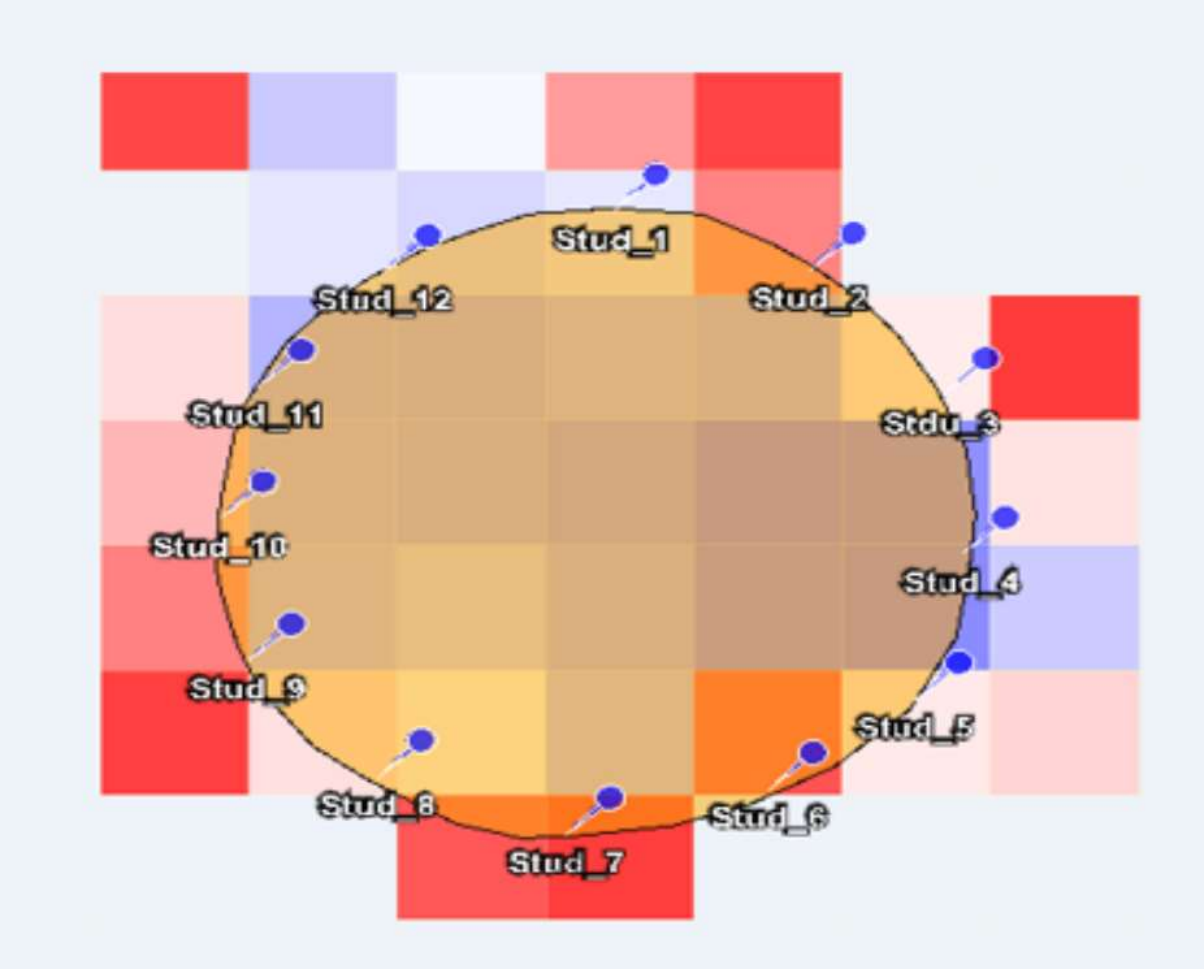

Figure 14: The image of the deformation of Tank 7 with STUD (12) captured around the crude oil storage tanks. (Source: [7]). Permission obtained to reuse image was obtained from the authors. Copyright year: 2022; Publisher: WJRR).

A typical geodetic X, Y, and Z deformation measurement is shown in Figure 15, which displays the values of the deformation. Similar to the previous example, the values of deformation range from -129.254mm to -122.6mm. Additionally, the level of deformation varies from one STUD to another,

and this variation is determined by the size of the bubble. The bubble plot of the retrieved deformation values on STUD positions on Tank 7 achieved through the use of the conventional geodetic technique is shown in Figure 15. Figure 16 depicts the bubble plot that was generated using the values of deformation that were taken from Tank 7. Between -29.669mm and -3.131mm is the range of values for the deformation metric. varied STUDs have varied levels of distortion, and the size of the bubble is what differentiates them from one another. A summarised table on the accuracy evaluation of the 10 oil storage tanks that were located within the study region is presented in Table 1.

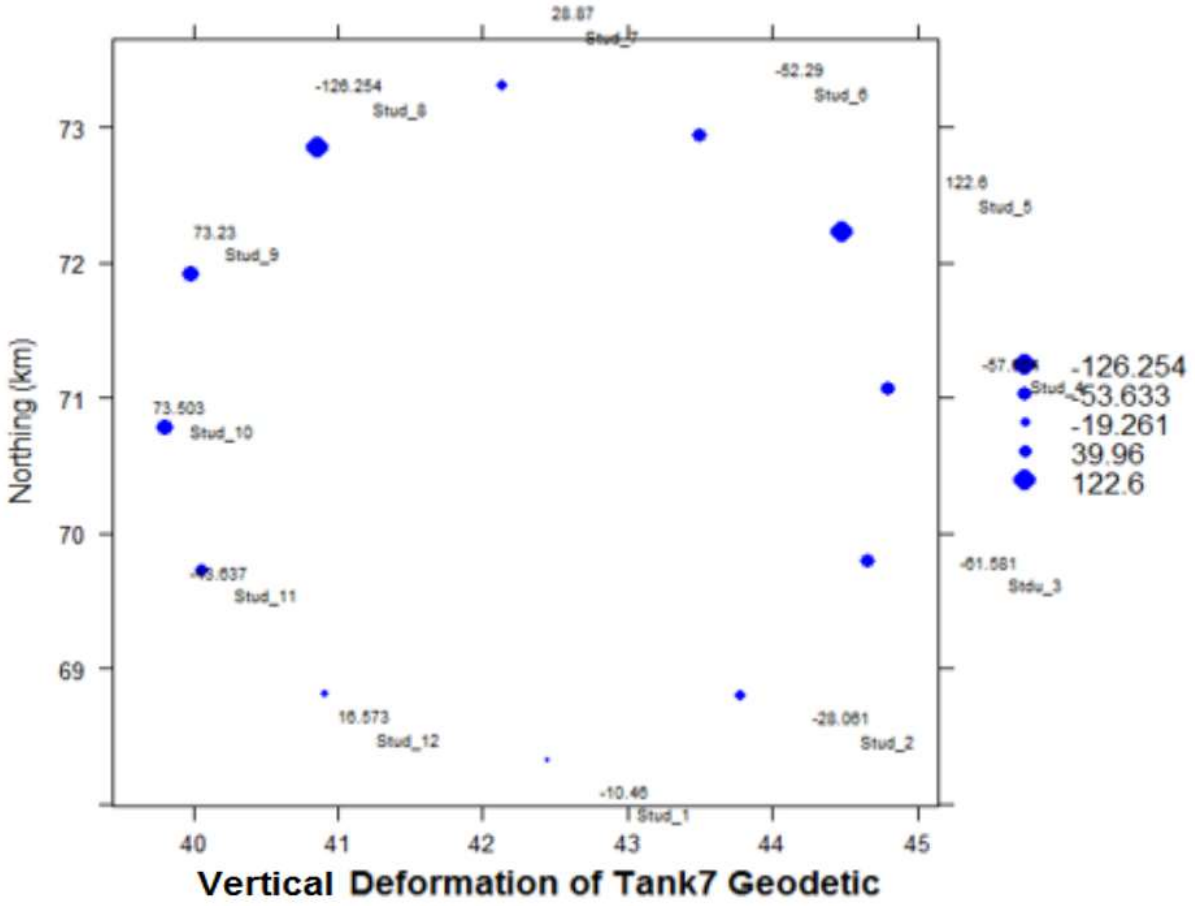

Figure 15: The bubble plot of the retrieved deformation values on STUD positions on Tank 7 achieved through the use of the conventional geodetic technique.

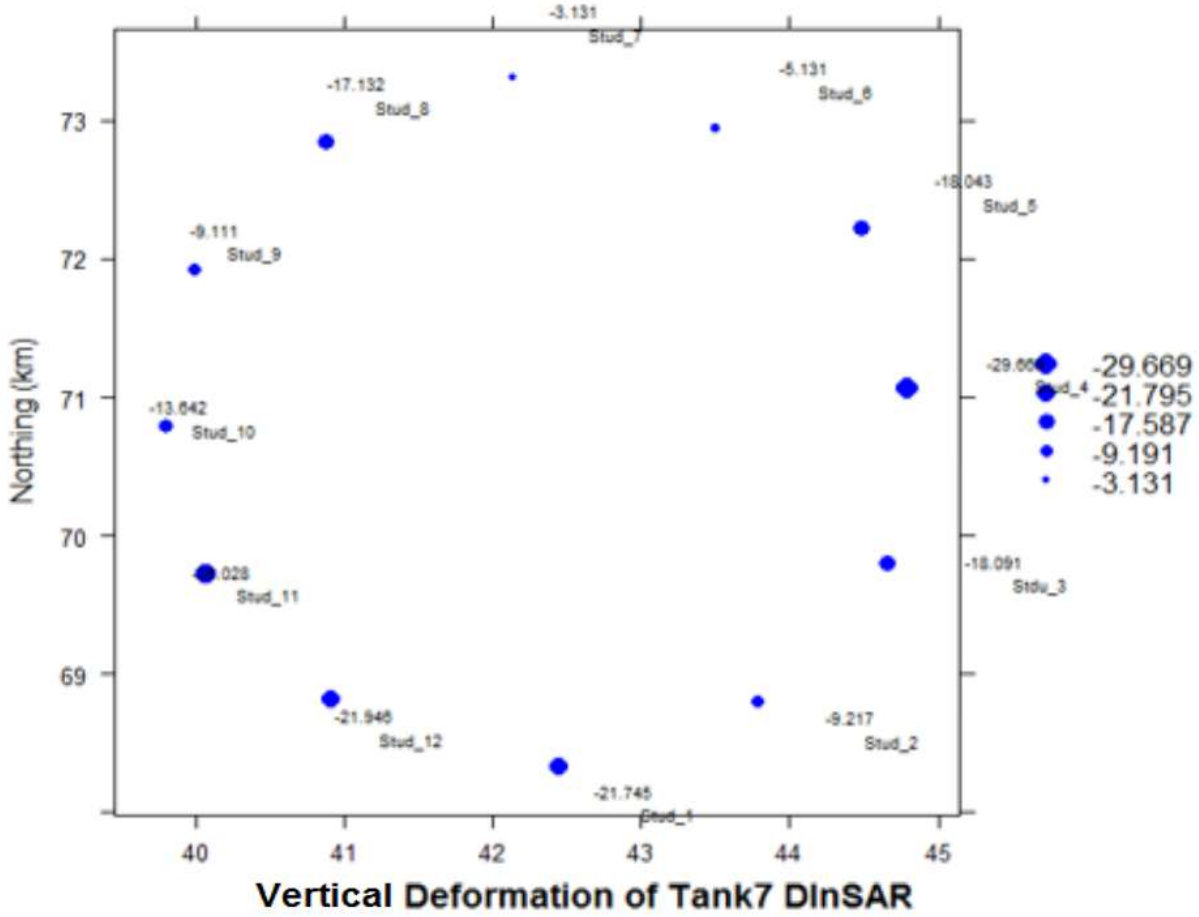

Figure 16: The bubble plot of the extracted deformation values on STUD locations on Tank 7 using the DInSAR technique.

Table 1: A summarised table on the accuracy evaluation of the 10 oil storage tanks that were located within the study region (Source: [7]). Permission obtained to reuse table was obtained from the authors. Copyright year: 2022; Publisher: WJRR).

Tank Number	Tank Observation	Percent of false positives	Percent of true positives
1	Deformed	4.154	95.846
2	Deformed	13.845	86.155
3	Deformed	79.287	20.712
4	Deformed	11.479	88.521
5	Deformed	78.367	21.633
6	Deformed	99.487	0.513
7	Deformed	30.765	69.235
8	Undeformed	100.000	100.000
9	Deformed	99.963	99.963
10	Deformed	4.566	4.566

The Results of the Statistical Analysis

The method of linear regression was utilised all throughout the statistical analysis. The linear regression tests are used to determine the relationship between the extracted deformation results from the DInSAR approach and the measured or computed deformation results from the classical geodetic technique. A statistical correlation plot of the extracted deformation values on STUD locations using DInSAR and the standard geodetic approach is shown in Figure 17.

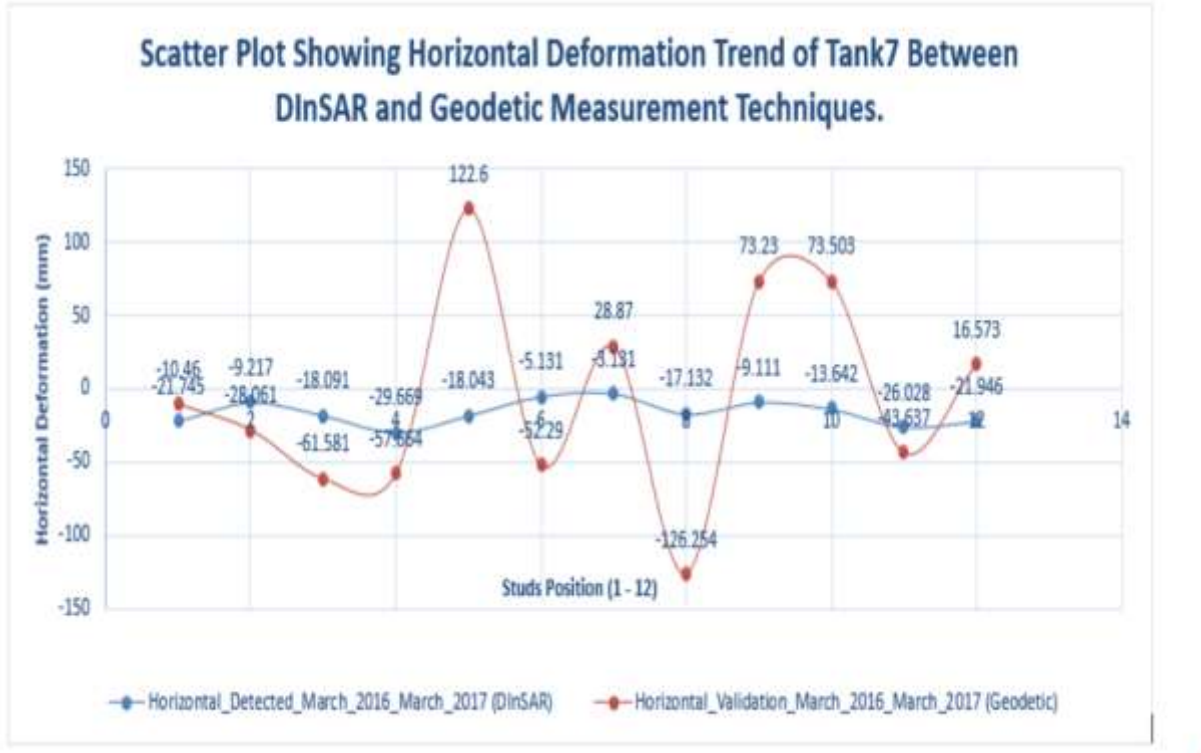

Figure 17: A statistical correlation plot of the extracted deformation values on STUD locations using DInSAR and the standard geodetic approach. (Source: [7]). Permission obtained to reuse image was obtained from the authors. Copyright year: 2022; Publisher: WJRR).

Also, another result in Figure 18 shows the vertical deformation plot from Studs around Tank 7 using (Geodetic) method. The deformation values ranges from (-18.664 mm – 8.87mm). It reflects the size of the bubbles differentiates the deformation on one Stud from another.

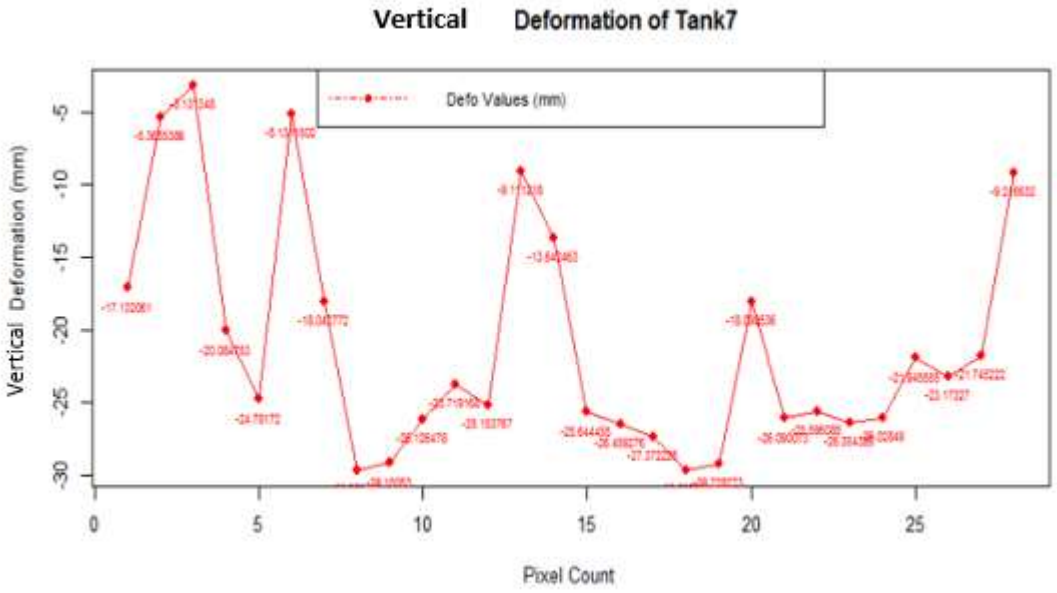

Figure 18: The graphical plot of vertical deformation around tank 7

Also, using the coordinates, the deformation values were validated using comparative analysis of the two approaches utilised. The coordinates of the studs around tank 7 which are 12 in number obtained using the traditional method (total station) and Interferometric synthetic Aperture Radar (see Figure 19).

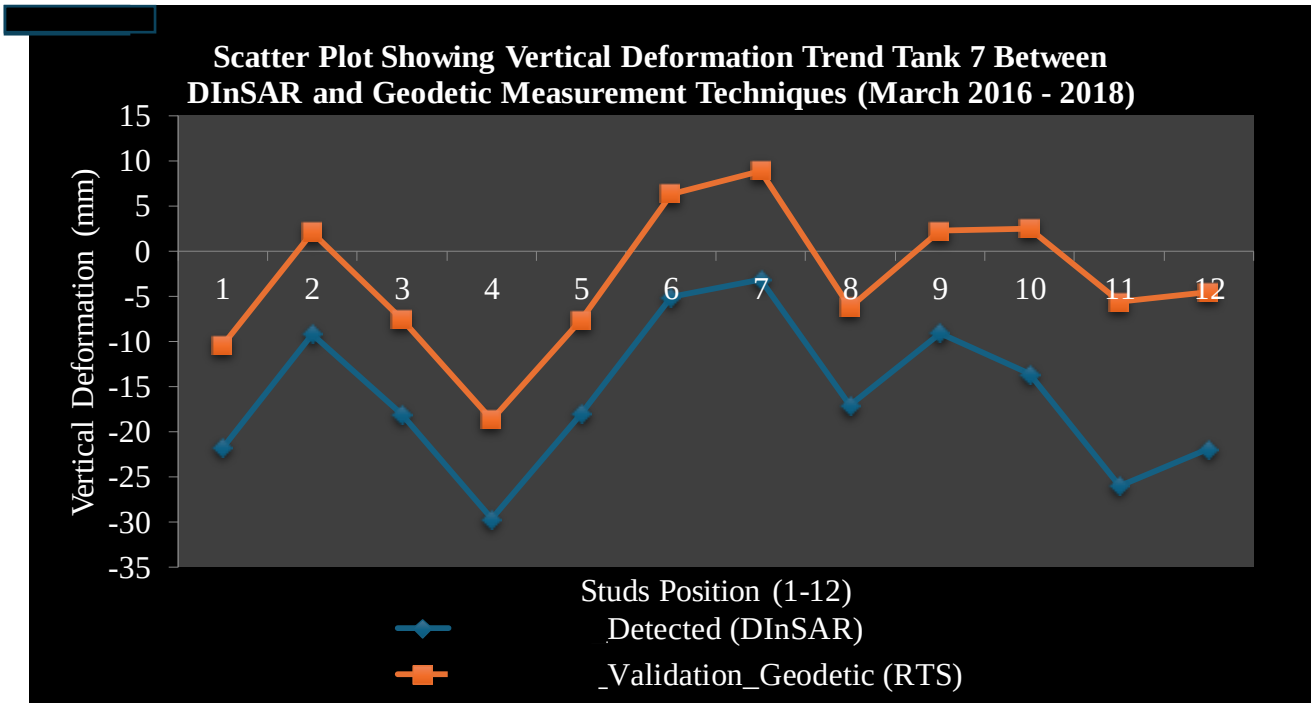

Figure 19: Comparative analysis between method (DInSAR) and Traditional Geodetic Measurements using a Scatter Plot

Discussions

According to the findings that are displayed in Figure 10, Tank 9 underwent a moderate amount of deformation, whilst Tanks 10,7,6,5,4,3,2 and Tank 1 underwent complete distortion, but Tank 8 definitely did not undergo any deformation at all. In Tank 8, the absence of deformation can be attributed to the fact that it was devoid of any contents and was not utilised during the time period under investigation. In addition, the coherence images that are displayed in Figures 12-13 provides unmistakable evidence that this is undergoing deformation. When compared to the black pixels in Figure 11, the bright pixels have an intensity of 1, whereas the black pixels have an intensity of 0. Additionally, the areas of distortion are displayed by the bright pixels, whereas the black pixels do not display any deformation. There are some tanks that fall into the white pixels, which indicate that they have deformed, but there are other tanks that fall into the black pixels, even though they have not deformed. The summary of the accuracy evaluation provides additional confirmation in Table 1 that there was radial displacement during the observation period at varied rates. Additionally, it reveals that there was a movement in the site of the greatest deformation magnitude. The sinking that has been seen is likely to be influenced by recent global warming as well as the rise in sea level that is linked with storm surge [3,4,18]. In addition, the non-uniform settlement of tank foundations, the loading and unloading of oil, and the temperature of the crude will all produce stress for the membrane of the tank [7,11]. It is also possible that the breakdown of the tank substrate by soluble sediments may lead to deformation [7,11,13]. This is because of the

poor monitoring, inspection, and maintenance techniques that have been implemented. However, a vertical deformation map with STUDS ranging from one to twelve is depicted in Figure 11, which is located around crude oil tank 7. These values of deformation were extracted with the help of this., as shown in Figure 20.

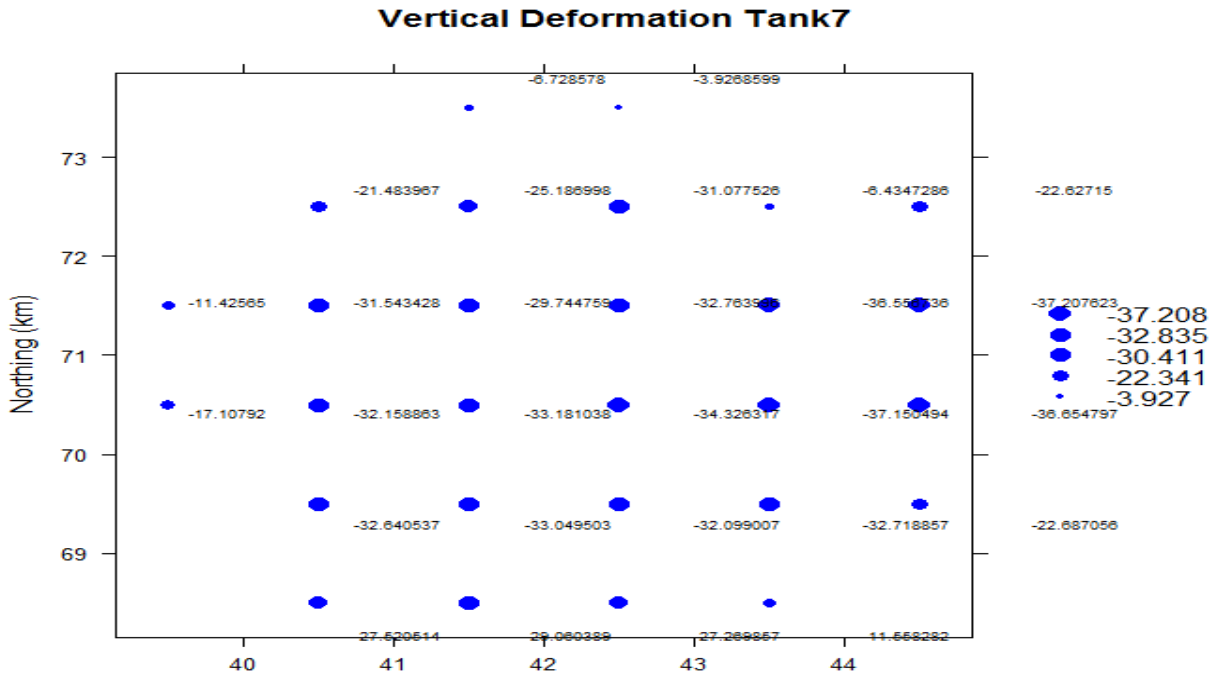

Figure 20: Bubble plot depicting vertical deformation of tank 7.

A plot of the vertical deformation that was obtained from Studs surrounding Tank 7 using geodetic methods is presented in Figure 15. From -126.254mm to 122.6mm, the values of the deformation span along this spectrum. Similarly, the vertical deformation plot from Studs surrounding Tank 7 is depicted in Figure 16, which was created using our approach (DInSAR). Between -29.669mm and -3.131mm is the range of values for the deformation process. It is possible to discern the deformation on one Stud from that of another based on the size of the bubbles. In a similar manner, the distinction between the deformations on one stud and another is determined by the size of the bubbles. The American Petroleum Institute (API) Standards state that even though some of the tanks have experienced deformation, none of the tanks should be taken out of service because the distortion is still within the acceptable range for safety.

As can be seen in Figures 17 and 19, there is a correlation that is not uniform between the classical geodetic measurement and the DinSAR. Both of the predicted DInSAR deformations are in the line of sight (LOS) direction of the SAR satellite, and the geodetic coordinates are in

reference to the position of the GPS [7,30]. The variations in pressure that occur as a consequence of the fluctuation within oil level are the cause of the fluctuations in vector direction that occur in both the DinSAR as well as geodetic measurements [14,31]. The DInSAR deformation trend is gradual, which is the pattern of deformation that is actually expected to occur in oil storage tanks (with the exception of extreme circumstances of external pressure). In oil storage tanks, the geodetic deformation trend is erratic and does not represent the expected deformation pattern in reality (it demonstrates a severe external pressure, which is extremely uncommon) [13,32]. It is possible that the mistake in the geodetic deformation trend is the result of the complexity of the mathematical model that was used to produce the results (this is still a particularly difficult problem in engineering geodesy). Based on the regression analysis, it appears that the horizontal distortions of the circular cross-section of tank 7 are deforming at a maximum line of sight (LOS) range of -3.131mm to -29.669mm per year for DInSAR, and -126.254mm to 122.6mm per year for the classic geodetic approach [7,33,34]. Lastly, in the earlier study by Nwodo et al. [7], the results were based on horizontal displacement, unlike the vertical displacements in this present study. However, since the storage tanks are circular in nature in both cases, the analysis confirms that both studies have deformations that present similar behaviours for the large oil storage tanks.

Conclusion

Large oil storage tanks that fail almost often result in fatalities, which can result in the loss of money, lives, and property, as well as the pollution of aquatic life and legal action, among other things. We established a system for periodic monitoring of these engineering structures in this study. The purpose of this monitoring was to determine the health of the structures as well as any substantial displacements from their original design specifications. The shortcomings of conventional geodetic methods for measuring oil storage tank deformations are addressed by our methodology, which reduces the expenditures, the level of difficulty, and the amount of time that is required. In addition to this, it proposes a solution that addresses the problem of oil spillage in Nigeria, which is caused by the failure of huge oil storage tanks and other engineering facilities. This approach involves the implementation of systematic monitoring. Despite the fact that the major objective of this research is not to provide a thorough structural deformation of the observed deformation, the simplified technique (supplementary information) does demonstrate the capability of observing the radial horizontal circular distortion that occurs in crude oil storage tanks. As a result, this cost-effective technique, which demonstrates a significant improvement over the conventional geodetic approach, will address a significant difficulty in the Nigerian oil sector and reduce the amount of global warming that is caused by oil pollution. Additionally, it will be efficient and helpful for the monitoring of safety risks associated with these oil tanks, particularly in developing nations that have fewer resources overall.

References

1. Ochege, F. U., Dike, E. C., & Okpala-Okaka, C. (2017). Geospatial assessment of vegetation status in Sagbama oilfield environment in the Niger Delta region, Nigeria. *Egyptian Journal of Remote Sensing and Space Science*, 20(2), 211-221. https://doi.org/10.1016/j.ejrs.2017.05.001
2. Dike E.C., Amaechi C.V., Beddu S.B., Weje I.I., Ameme B.G., Efeovbokhan O., Oyetunji A.K. (2024). Coastal Vulnerability Index sensitivity to shoreline position and coastal elevation parameters in the Niger Delta region, Nigeria. *Sci Total Environ.* 2024 Apr 1;919:170830. https://doi.org/10.1016/j.scitotenv.2024.170830.
3. Dike, E. C., Oyetunji, A. K., Amaechi, C. V., & Pattiaratchi, C. (Ed.) (2023). Shoreline Delineation from Synthetic Aperture Radar (SAR) Imagery for High and Low Tidal States in Data-Deficient Niger Delta Region. *Journal of Marine Science and Engineering (JMSE),* 11(8), Article 1528. https://doi.org/10.3390/jmse11081528
4. Obida, C. B., Blackburn, G. A., Whyatt, J. D., & Semple, K. T. (2019). River network delineation from Sentinel-1 SAR data. *International Journal of Applied Earth Observation and Geoinformation*, *83*, 101910. https://doi.org/10.1016/j.jag.2019.101910
5. Obida, C. B., Blackburn, G. A., Whyatt, J. D., & Semple, K. T. (2021). Counting the cost of the Niger Delta's largest oil spills: Satellite remote sensing reveals extensive environmental damage with> 1million people in the impact zone. *Science of the Total Environment*, *775*, 145854. https://doi.org/10.1016/j.scitotenv.2021.145854
6. Obida, C. B., Blackburn, G. A., Whyatt, J. D., & Semple, K. T. (2018). Quantifying the exposure of humans and the environment to oil pollution in the Niger Delta using advanced geostatistical techniques. *Environment international*, *111*, 32-42. https://doi.org/10.1016/j.envint.2017.11.009
7. Nwodo, G. O., Okeke, F. I., & Nduji, N. N. (2022). Application of Interferometric Synthetic Aperture Radar (InSAR) Technique in Monitoring the Deformation of Large Oil Storage Tanks. *World Journal of Research and Review*, *15*(6), 18-25. https://doi.org/10.31871/WJRR.15.6.6
8. Eboh, M. (2016). Nigeria: NNPC Raises Petrol Storage Capacity By 87.7 Million Litres. The Vanguard. Published on 29 September 2016. Publisher: Vanguard (Lagos). Available at: https://allafrica.com/stories/201609290194.html Accessed on 3rd August, 2024
9. EgyptOil (2016). Nigeria Enhanced Fuel Storage. Published on 3rd October 2016 by Egypt Oil & Gas. Available at: https://egyptoil-gas.com/news/nigeria-enhanced-fuel-storage/ Accessed on 3rd August, 2024
10. Wittels, J. and Lehane, B. (2024). Nigeria's Giant New Oil Refinery Posts Videos of Fuel Loadings. Published on 15 April 2024 by Bloomberg. Available at: https://www.bloomberg.com/news/articles/2024-04-15/nigeria-s-giant-new-oil-refinery-posts-videos-of-fuel-loadings Accessed on 3rd August, 2024
11. Ehigiator, M. O.and Ehigiator–Irughe, R. (2018). Formulation and Implementation of Mathematical Models Suitable for Deformation Analysis of Structures. Nigerian Journal of Technology, Vol. 37(2), pp. 294 – 301.
12. Gairns, C. (2008). Development of semi-automated system for structural deformation monitoring using a reflector less total station. M.Sc. Thesis. – Department of Geodesy and Geomatics Engineering – University of New Brunswick.
13. Irughe – Ehigiator, R., Ehiorobo, J.O., Beshir, A. A., andEhigiator, M.O. (2012). Determination of the Ovality of Crude Oil Storage Tanks using Least Squares. Advanced

Materials Research, Vol. 367 (2012), pp. 475-483. doi:10.4028/www.scientific.net/AMR.367.475
14. Irughe – Ehigiator, R., Ehiorobo, J.O., Ehigiator, M.O., and Beshir, A. A. (2012). Determining the Subsidence of Oil Storage Tank Walls from Geodetic Leveling. Advanced Materials Research, Vol. 367 (2012), pp. 467-474.
15. Di Martire, D.; Tessitore, S.; Brancato, D.; Ciminelli, M.G.; Costabile, S.; Costantini, M.; Graziano, G.V.; Minati, F.; Ramondini, M.; Calcaterra, D. Landslide detection integrated system (LaDIS) based on in-situ and satellite SAR interferometry measurements. Catena 2016, 137, 406–421. https://doi.org/10.1016/j.catena.2015.10.002.
16. Strozzi, T.; Wegmiiller, U.; Tosl, L.; Bitelli, G.; Spreckels, V. Land Subsidence Monitoring with Differential SAR Interferometry. Photogramm. Eng. Remote Sens. 2001, 67, 1261–1270.
17. Poulsen, B. A.; Shen, B. Surface Subsidence from Underground Coal Mining Impacting Residential Housing: A Case Study of Risk Analysis, Mitigation Proposal and Ongoing MonitorinG. WIT Trans. Eng. Sci. 2018, 121, 209–220. https://doi.org/10.2495/RISK180181.
18. Casu, F., Elefante, S., Imperatore, P., Zinno, I., & Manunta, M. (2014). SBAS-DInSAR Parallel Processing for Deformation Time-Series Computation, August https://doi.org/10.1109/JSTARS.2014.2322671
19. Raspini, F.; Bianchini, S.; Ciampalini, A.; Del Soldato, M.; Solari, L.; Novali, F.; Del Conte, S.; Rucci, A.; Ferretti A.; Casagli, N. Continuous, semi-automatic monitoring of ground deformation using Sentinel-1 satellites. Sci. Rep. 2018, 8, 7253. doi:10.1038/s41598-018-25369-w.
20. Mahour, M., Tolpekin, V., & Stein, A. (2016). Tree detection in orchards from VHR satellite images using scale-space theory, 10004, 1–17. https://doi.org/10.1117/12.2241529.
21. Clinton, N., Holt, A., Scarborough, J., Yan, L., & Gong, P. (2010). Accuracy assessment measures for object-based image segmentation goodness. Photogrammetric Engineering & Remote Sensing, 76(3), 289–299. https://doi.org/10.14358/PERS.76.3.289.
22. Nduji, N. N. (2017). Super resolution mapping of trees from satellite images at different scales.
23. Luca, C. De, Cuccu, R., Elefante, S., Zinno, I., Manunta, M., Casola, V., … Casu, F. (2015). An On-Demand Web Tool for the Unsupervised Retrieval of Earth's Surface Deformation from SAR Data: The P-SBAS Service within the ESA G-POD Environment, 15630–15650. https://doi.org/10.3390/rs71115630.
24. Hay, G. J., & Castilla, G. (2006). Object-based image analysis: strengths, weaknesses, opportunities and threats (SWOT). International Archives of Photogrammetry Remote Sensing and Spatial Information Sciences, 36, 4. Retrieved from http://www.isprs.org/proceedings/XXXVI/4-C42/Papers/01_OpeningSession/OBIA2006_Hay_Castilla.pdf. (accessed on 3rd August 2024).
25. Blaschke, T. (2010). Object based image analysis for remote sensing. ISPRS Journal of Photogrammetry and Remote Sensing, 65(1), 2–16. https://doi.org/10.1016/j.isprsjprs.2009.06.004
26. Baglioni, M., Antônio, J., Macêdo, F. De, & Renso, C. (2009). Advances in GIScience. (B. Thomas, H. Geoffrey, & S. Lang, Eds.), Notes. Berlin Heidelberg: Springer Berlin Heidelberg. https://doi.org/10.1007/978-3-642-00318-9

27. Blaschke, T., Hay, G. J., Kelly, M., Lang, S., Hofmann, P., Addink, E., … Tiede, D. (2014). Geographic Object-Based Image Analysis - Towards a new paradigm. ISPRS Journal of Photogrammetry and Remote Sensing, 87, 180–191. https://doi.org/10.1016/j.isprsjprs.2013.09.014.
28. Chen, Y.; Wang, K. Accuracy verification and evaluation of Sentinel-1A repeat track differential interferometric synthetic aperture radar in monitoring mining subsidence. J. Appl. Remote Sens. 2021, 14, 014501. https://doi.org/10.1117/1.JRS.14.
29. Ferretti, A.; Monti-guarnieri, A.; Prati, C.; Rocca, F. InSAR Principles: Guidelines for SAR Interferometry Processing and Interpretation. 2007. Available online: https://www.esa.int/esapub/tm/tm19/TM-19_ptA.pdf (accessed on 3rd August 2024).
30. Engelbrecht, J. and Inggs, M. (2013). Differential Interferometry Techniques on L-Band Data Employed for the Monitoring of Surface Subsidence Due to Mining. South African Journal of Geomatics, Vol. 2 (2).
31. Erol, S., Erol, B., and Ayan, T. (2004). A General Review of the Deformation Monitoring Techniques and A Case Study: Analysing Deformations Using Gps/Levelling.
32. Pantousa, D. (2015). Numerical Simulation of Oil Steel Tank Structural Behavior Under Fire Conditions. A Master Thesis Submitted to the Department of Mechanical Engineering, University of Thessaly.
33. Pukanská, K., Gajdošík, J., Marcian, M., and Bartoš, K. (2014). Determination of Deformations of a High-Capacity Tank Using the Technology of Terrestrial Laser Scanning. American International Journal of Contemporary Research, Vol. 4 (4), pp. 38 – 45.
34. Reeves, J. A. (2013). Using Interferometric Synthetic Aperture Radar Data to Improve Estimates of Hydraulic Head in The San Luis Valley, Colorado. A PhD Dissertation Submitted to The Department of Geophysics and The Committee On Graduate Studies of Stanford University.

